NJC

Accepted Manuscript

This is an *Accepted Manuscript*, which has been through the Royal Society of Chemistry peer review process and has been accepted for publication.

Accepted Manuscripts are published online shortly after acceptance, before technical editing, formatting and proof reading. Using this free service, authors can make their results available to the community, in citable form, before we publish the edited article. We will replace this *Accepted Manuscript* with the edited and formatted *Advance Article* as soon as it is available.

You can find more information about *Accepted Manuscripts* in the Information for Authors.

Please note that technical editing may introduce minor changes to the text and/or graphics, which may alter content. The journal's standard Terms & Conditions and the Ethical guidelines still apply. In no event shall the Royal Society of Chemistry be held responsible for any errors or omissions in this *Accepted Manuscript* or any consequences arising from the use of any information it contains.

ROYAL SOCIETY OF CHEMISTRY

www.rsc.org/njc

NJC

RSCPublishing

LETTER

Facile approach to prepare $Bi(OH)_3$ nanoflakes as high-performance pseudocapacitor material

Cite this: DOI: 10.1039/c3nj00000x

Wei Zhang,[a] Xiaoxiong Huang,[a] Yueyue Tan,[a] Yilong Gao,[a] Jianxiang Wu,[a] Jinbo Hu,[b] Andreas Stein [b] and Bohejin Tang [a,b,*]

Received 00th XXXXX 2013,
Accepted 00th XXXXX 2013

DOI: 10.1039/c3nj00000x

www.rsc.org/njc

Abstract: $Bi(OH)_3$ nanoflakes are prepared by a facile one-step solvothermal approach. The product has a porous structure built up of many interconnected nanoflakes with a thickness of approximately 20 nm. The $Bi(OH)_3$ nanoflakes deliver a specific capacitance of 888 F g^{-1} at current densities of 1 A g^{-1}.

Electrochemical capacitors (ECs) have attracted much research interests in recent years because of their high power density, excellent reversibility, and long-cycle life.[1] Electrochemical capacitors are based on two principal types of capacitive behavior: one associated with an electrochemical double layer (EDL) at electrode-electrolyte interfaces and another associated with pseudocapacitance. Carbon materials with high specific surface areas and good electrical conductivity are usually used as electrodes in electrochemical double layer capacitors (EDLCs).[2, 3] However, the specific capacitance of EDLCs is limited and far from satisfactory in accordance with the ever-growing need for practical usages. In pseudocapacitors, on the other hand, energy is stored through a reversible adsorption of small-size ions and redox reactions occurring on the surface as well as in the bulk materials. These two contributions result in higher capacitance and energy density compared to EDLCs.[4] Among the variety of pseudocapacitive materials, transition metal oxides are some of the most studied electrodes materials, due to ther high theoretical capacity, environmental stability and interesting electroactivity. For example, electrodes composed of hydrous RuO_2 nanotubular array exhibit unexpectedly ultrahigh power characteristics.[5] However, their high cost has impeded their usage in practical applications. A number of transition metal oxides have been studied as alternative electrodes such as MnO_2,[6, 7] Co_3O_4,[8, 9] Fe_2O_3,[10] NiO,[11, 12] and CuO[13] in aqueous or non-aqueous solutions.

In recent years, due to its high electrochemical stability, high redox reversibility, and relatively high power and capacity, bismuth oxides have received significant attention as electrode material.[14-16] For example, Gujar et al.[17] reported Bi_2O_3 as a supercapacitor electrode material with pseudo-capacitance, but the specific capacitance of a Bi_2O_3 thin film prepared by electro-deposition was only 98 F g^{-1}. Xia et al.[16] synthesized worm-like mesoporous carbon@Bi_2O_3 composites by an efficient and fast microwave method. The composites exhibited excellent capacitance performance with a maximum specific capacitance of 386 F g^{-1}, three times more than that of the pure worm-like mesoporous carbon. Hu et al.[18] demonstrated a novel and facile route for preparing graphene-based composites comprising metal oxide nanoparticles and graphene. Bismuth oxide-loaded graphene achieves a specific capacitance as high as 825 F g^{-1} at 1 A g^{-1}. In the present work we report for the first time, to the best of our knowledge, the pseudocapacitive behavior of a $Bi(OH)_3$-based electrode.

In our work, the preparation of $Bi(OH)_3$ nanoflakes was conducted by a facile one-step solvothermal method. As can be clearly seen in scanning electron microscopy (SEM) images (Fig. 1a and 1b), $Bi(OH)_3$ exhibits a nanoflake-like structure with a flake thickness of about 20 nm. It is noteworthy that the product morphology, which consists of interconnected irregular nanoflakes, may be potentially significant for the electrochemical performance of the material. For further investigation of the inner structure, transmission electron microscopy (TEM) was employed. TEM images of $Bi(OH)_3$ in Fig. 1c and 1d clearly display the ultrathin flake structure of the materials, also showing a nanoflake thickness of about 20 nm, in good agreement with the results from the SEM images. The crystal phase and structure information of the samples was obtained by powder X-ray diffractions (PXRD) measurement. Fig. 2 shows the XRD pattern of the $Bi(OH)_3$, which coincides with the standard pattern for $Bi(OH)_3$ (JCPDS: 01-0898). The BET surface area and the porosity properties of the electrode materials are

important parameters governing the pseudocapacitor performance. The sorption isotherm of the $Bi(OH)_3$ flakes (Fig. 3) shows type IV characteristics with a narrow hysteresis for $Bi(OH)_3$. The sample exhibits a BET surface area of 27.2 m^2 g^{-1} and a pore volume of 0.149 cm^3 g^{-1}. The pore size distribution is centered around 2 nm, as calculated from desorption data using the BJH model.

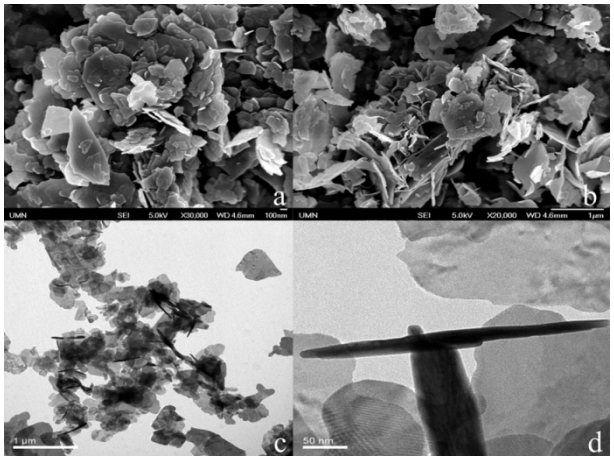

Fig. 1. SEM (a and b) and TEM (c and d) micrographs of $Bi(OH)_3$.

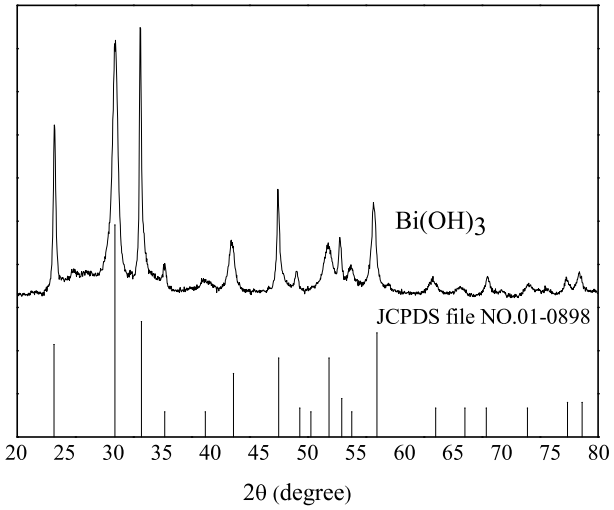

Fig. 2. XRD patterns of the $Bi(OH)_3$ nanoflakes.

It can be seen that a pair of redox peaks are visible in each cyclic voltammetry (CV) curve, suggesting that the measured capacitance is mainly based on the redox mechanism, confirming the pseudocapacitive behavior of the $Bi(OH)_3$. Based on previous reports, the charge transfer mechanism following this electrochemical process can be described by the chemical reactions below. In the cathodic scan, peak C (Fig. 4a) is ascribed to the following reaction in a KOH electrolyte[19, 20]:

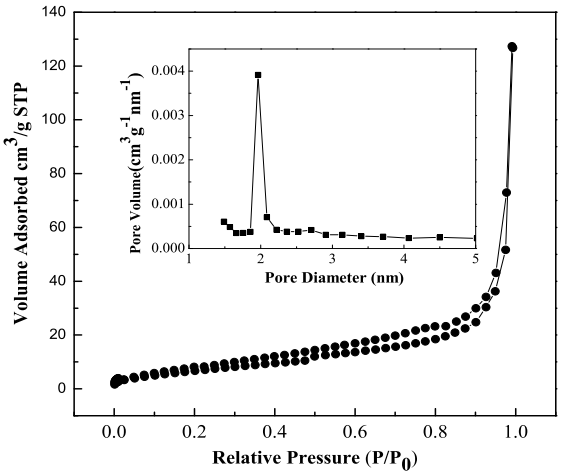

Fig. 3. Nitrogen adsorption and desorption isotherms and pore-size distribution curves (inset) of the $Bi(OH)_3$ nanoflakes.

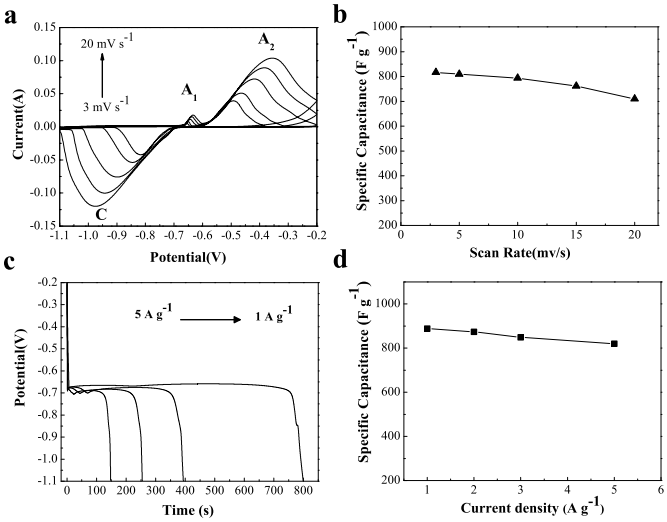

Fig. 4. (a) The cyclic voltammetry curves of $Bi(OH)_3$-based electrodes at an increasing voltage scanning rate of 3, 5, 10, 15 and 20 mV s^{-1}; the potential is given vs. a saturated calomel electrode (SCE) (b) Specific capacitance of $Bi(OH)_3$-based electrodes at different scan rates. (c) Discharge curves of $Bi(OH)_3$-based electrodes at different current densities of 1, 2, 3 and 5 A g^{-1}; (d) Specific capacitance of $Bi(OH)_3$-based electrodes at various discharge current densities.

$$Bi(OH)_3 + OH^- \rightarrow BiO_2^- + 2H_2O$$
$$BiO_2^- + 2H_2O + 3e^- \rightarrow Bi + 4OH^-$$

In the anodic step, peak A_1 (Fig. 4a) has been attributed to the oxidation of cathodically formed Bi [21],

$$Bi + 4OH^- \rightarrow BiO_2^- + 2H_2O + 3e^-$$

whereas peak A_2 (Fig. 4a) has previously been assigned to the oxidation:

$$Bi + 3OH^- \rightarrow Bi(OH)_3 + 3e^-$$

From the CV, the specific capacitance can be estimated as follows[22]:

$$C = \frac{1}{2 \times v \times \Delta m \times \Delta V} \int I \, dV$$

where C is the specific capacitance (F g^{-1}), v is the scan rate (V/s), Δm is the mass of the active material (g), ΔV is the potential window (V) and I dV represents the area under CV curve (Q). The average specific capacitance of the $Bi(OH)_3$ composite was calculated to be 816, 808, 793, 760 and 710 F g^{-1} at scan rates of 3, 5, 10, 15 and 20 mV s^{-1} (Fig. 4b), respectively. The ultrathin nanoflakes of $Bi(OH)_3$ provide the high activity, which helps to improve the specific capacitance. In addition, the peaks of CVs are almost symmetrical throughout the whole range of scan rates (Fig. 4a), which suggest the reversibility of the oxidation and reduction steps. Furthermore, the high reversibility in processes is also beneficial to the cycling stability of $Bi(OH)_3$ electrode. However, the specific capacitance of the composite electrode decreased with increasing scan rate. At lower scan rates, the diffusion of ions from the electrolyte can enter almost all the effective pores of the electrode. With higher scan rates, the effective interaction between the ions and the electrode is greatly reduced, which led to a lower specific capacitance. At these higher rates, the active material at the inner surface may not be fully involved in the electrochemical process due to the limited ion diffusion.[7, 23]

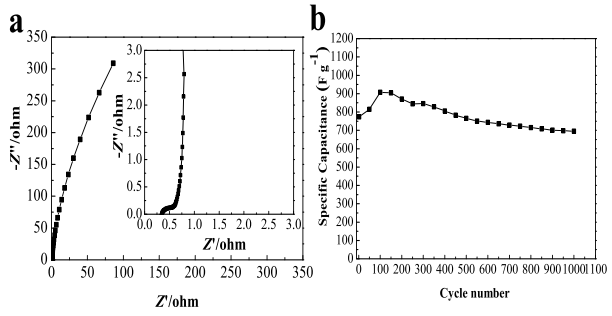

Fig. 5. (a) Impedance spectra of $Bi(OH)_3$ (inset is the magnification of the Nyquist curve); Z' is real impedance. Z'' is imaginary impedance. (b) Cycling performance of $Bi(OH)_3$ at a scan rate of 10 m V^{-1}.

Galvanostatic charge-discharge measurement was also used to evaluate the capacitance behavior of $Bi(OH)_3$. Fig.4(c) describes the galvanostatic discharge of the $Bi(OH)_3$ in 6 *M* KOH solution over the potential range from −1.1 V to -0.2 V at different current densities of 1, 2, 3 and 5 A g^{-1}.The nonlinear behavior of the voltage-time curves in Fig.4(c) is expected for pseudocapacitive electrodes. The specific capacitance can be calculated from the galvanostatic charge-discharge curve according to equation[24]:

$$C = \frac{I \times \Delta t}{\Delta m \times \Delta V}$$

where C is the specific capacitance (F g^{-1}), I is the current (A), Δt is the discharge time (s), ΔV is the potential window (V) and Δm is mass of the electroactive material (g). The specific capacitance of the $Bi(OH)_3$ nanoflakes reached 888 F g^{-1} at 1 A g^{-1}. At a current density of 5 A g^{-1}, 92% of this specific capacitance is retained, indicating the high-rate capabilities of the $Bi(OH)_3$ nanoflakes. From Fig. 4(b) and 4(d), we conclude that the morphology of the $Bi(OH)_3$ electrode material is favorable for fast ion diffusion and electron transfer reaction especially at high current density.

In addition, electrochemical impedance spectroscopy (EIS) analysis was conducted in order to better understand the remarkable electrochemical behavior. As shown in Fig. 5(a) the Nyquist plot contains a semicircle in high frequency region and a nearly vertical line in the low frequency region. Generally, the semicircle is considered to be the charge transfer resistance at the electrode/electrolyte interface,[25] indicating the small charge transfer resistance. At low frequencies, the electrode has an ideal straight-line behavior along the imaginary axis, indicating low Warburg impedance (W) and low electrolyte diffusion resistance favourable for capacitive performance. The resistance of the $Bi(OH)_3$-based electrode was close to 0.4 Ω. Good cycling stability is another important characteristic for a high performance pseudocapacitor. Fig. 5(b) shows that the specific capacitance increased during the first 120 cycles, which resulted from an activation process for the $Bi(OH)_3$ electrode. After this process, the $Bi(OH)_3$ electrode still maintained a capacitance of about 700 F g^{-1} (about 90 % of the initial capacitance) after 1000 cycles.

These results revealed that these $Bi(OH)_3$ nanoflakes with a thickness of sizes about 20 nm prepared by a facile solvothermal method are suitable materials for electrochemical pseudocapacitors. The obtained $Bi(OH)_3$ exhibited excellent electrochemical capacitive performance. A high specific capacitance of 888 F g^{-1} was achieved at a current density of 1 A g^{-1} and 90% (700 F g^{-1}) of the initial specific capacitance remained after 1000 cycles. Taking advantage of ther high performance, cycle stability, easy fabrication and low-cost, it is believed that the prepared $Bi(OH)_3$ nanoflakes demonstrate a design for next-generation pseudocapacitor electrode material.

Experimental

Material Synthesis

A typical experimental procedure is as follows: 0.136 g of sodium acetate trihydrate ($CH_3COONa \cdot 3H_2O$) was dissolved in deionized water (10 mL) by ultrasonication (denoted as sample 1). Separately, a solution of 0.486 g $Bi(NO_3)_3 \cdot 5H_2O$ and 25 mL glycol was mixed for 10 min. Sample 1 was added to this solution, and the mixture was sonicated for another 30 min. The whole mixture was then transferred into a polytetrafluoroethylene (PTFE)-lined autoclave and maintained at 180 ° C for 12 h. After natural cooling to room temperature, the precipitates were collected by centrifugation, thoroughly washed 6 times with ethanol, and then dried in an oven at 60 ° C for 12 h to obtain white powders of $Bi(OH)_3$.

Electrochemical measurements

Electrodes for electrochemical performance were constructed by mixing active material, carbon black and poly tetrafluoroethylene (PTFE) binder with a weight percent ratio of 75:20:5. The mixture was dispersed in ethanol and pressed onto nickel foams under a pressure of 12 MPa. The geometric surface area of the prepared working electrode was 1 cm^2. The electrodes were dried under vacuum at 90 °C for 1 h to remove the solvent. Nickel foam (1.6 mm thick, 95% purity, Goodfellow) was used as a current collector.

The electro-chemical measurements were carried out using CHI 660D electrochemical workstation (Shanghai Chen Hua, Inc.). The conventional three-electrode cell was equipped with a Pt plate as the counter electrode and a saturated calomel electrode (SCE) as the reference electrode. CV tests were performed within the range of -1.1 and -0.2 V, using scan rates of 5, 10 and 20 mV s^{-1}. EIS measurements were carried out in the frequency range of 100 kHz to 0.01 Hz. All experiments were carried out at a room temperature and in 6 *M* KOH solution.

Compositional and Structural Characterization

Powder X-ray diffractions (XRD) patterns of the samples were performed obtained using a D/Max-RB diffractometer with Cu-Kα radiation (λ=1.54056 Å) and a graphite monochromator at 50 kV, 100 mA. The particle sizes and morphologies of the powders were observed by transmission electron microscopy (TEM) on Hitachi H-800 microscope and scanning electron microscopy (SEM) on JEOL-6700 microscope operating at 5 kV. N_2 adsorption–desorption isotherms were measured using a Micromeritics ASAP 2460 analyzer at 77 K; the Brunauer-Emmett-Teller (BET) method was utilized to calculate the specific surface areas and pore size distributions were calculated from desorption isotherms using the Barett-Joyner-Halenda (BJH) model.

Acknowledgements

A part of this work was supported by the University of Minnesota Initiative for Renewable Energy and the Environment (IREE). Parts of this work were carried out in the Characterization Facility, University of Minnesota, which receives partial support from NSF through the MRSEC program.

Notes and references

a College of Chemistry and Chemical Engineering, Shanghai University of Engineering Science, Shanghai 201620, PR China
b Department of Chemistry, University of Minnesota, 207 Pleasant St. SE, Minneapolis, Minnesota 55455, United States
E-mail: tangbohejin@sues.edu.cn (Bohejin Tang)

1. L.-Q. Mai, A. Minhas-Khan, X. Tian, K. M. Hercule, Y.-L. Zhao, X. Lin and X. Xu, *Nature communications*, 2013, 4.
2. D. Yu and L. Dai, *The Journal of Physical Chemistry Letters*, 2009, 1, 467-470.
3. H.-J. Liu, X.-M. Wang, W.-J. Cui, Y.-Q. Dou, D.-Y. Zhao and Y.-Y. Xia, *J. Mater. Chem.*, 2010, 20, 4223-4230.
4. P. Sharma and T. Bhatti, *Energy Conversion and Management*, 2010, 51, 2901-2912.
5. C.-C. Hu, K.-H. Chang, M.-C. Lin and Y.-T. Wu, *Nano Lett.*, 2006, 6, 2690-2695.
6. M. Xu, L. Kong, W. Zhou and H. Li, *The Journal of Physical Chemistry C*, 2007, 111, 19141-19147.
7. V. Subramanian, H. Zhu, R. Vajtai, P. Ajayan and B. Wei, *The Journal of Physical Chemistry B*, 2005, 109, 20207-20214.
8. J. Liu, J. Jiang, C. Cheng, H. Li, J. Zhang, H. Gong and H. J. Fan, *Adv. Mater.*, 2011, 23, 2076-2081.
9. X.-H. Xia, J.-P. Tu, X.-L. Wang, C.-D. Gu and X.-B. Zhao, *Chemical Communications*, 2011, 47, 5786-5788.
10. D. Sarkar, G. G. Khan, A. K. Singh and K. Mandal, *The Journal of Physical Chemistry C*, 2013, 117, 15523-15531.
11. X.-h. Xia, J.-p. Tu, X.-l. Wang, C.-d. Gu and X.-b. Zhao, *J. Mater. Chem.*, 2011, 21, 671-679.
12. S. K. Meher, P. Justin and G. R. Rao, *Nanoscale*, 2011, 3, 683-692.
13. X. Zhang, W. Shi, J. Zhu, D. J. Kharistal, W. Zhao, B. S. Lalia, H. H. Hng and Q. Yan, *ACS Nano*, 2011, 5, 2013-2019.
14. D. Yuan, J. Zeng, N. Kristian, Y. Wang and X. Wang, *Electrochemistry Communications*, 2009, 11, 313-317.
15. F.-L. Zheng, G.-R. Li, Y.-N. Ou, Z.-L. Wang, C.-Y. Su and Y.-X. Tong, *Chem. Commun.*, 2010, 46, 5021-5023.
16. N. Xia, D. Yuan, T. Zhou, J. Chen, S. Mo and Y. Liu, *Materials Research Bulletin*, 2011, 46, 687-691.
17. T. Gujar, V. Shinde, C. Lokhande and S.-H. Han, *Journal of power sources*, 2006, 161, 1479-1485.
18. H.-W. Wang, Z.-A. Hu, Y.-Q. Chang, Y.-L. Chen, Z.-Q. Lei, Z.-Y. Zhang and Y.-Y. Yang, *Electrochimica Acta*, 2010, 55, 8974-8980.
19. V. Vivier, C. Cachet‐Vivier, S. Mezaille, B. Wu, C. Cha, J. Y. Nedelec, M. Fedoroff, D. Michel and L. Yu, *Journal of The Electrochemical Society*, 2000, 147, 4252-4262.
20. R. Pauliukaite, R. Metelka, I. Švancara, A. Królicka, A. Bobrowski, K. Vytřas, E. Norkus and K. Kalcher, *Analytical and bioanalytical chemistry*, 2002, 374, 1155-1158.
21. A. Espinosa, M. San José, M. Tascón, M. Vázquez and P. S. Batanero, *Electrochimica acta*, 1991, 36, 1561-1571.
22. V. Nithya, R. Kalai Selvan, D. Kalpana, L. Vasylechko and C. Sanjeeviraja, *Electrochim. Acta*, 2013, 109, 720-731.
23. M.-W. Xu, D.-D. Zhao, S.-J. Bao and H.-L. Li, *J. Solid State Electrochem.*, 2007, 11, 1101-1107.
24. B. Hu, X. Qin, A. M. Asiri, K. A. Alamry, A. O. Al-Youbi and X. Sun, *Electrochim. Acta*, 2013, 107, 339-342.
25. Y. Wang, Z. Shi, Y. Huang, Y. Ma, C. Wang, M. Chen and Y. Chen, *The Journal of Physical Chemistry C*, 2009, 113, 13103-13107.

